Interplay of *Mycobacterium abscessus* and *Pseudomonas aeruginosa* in coinfection: Biofilm Dynamics and Host Immune Response

Víctor Campo-Pérez[1,2], Esther Julián[2,*] and Eduard Torrents[1,3,*]

[1] Bacterial Infections and Antimicrobial Therapy Group, Institute for Bioengineering of Catalonia (IBEC), The Barcelona Institute of Science and Technology (BIST), Baldiri Reixac 15-21, 08028 Barcelona, Spain.

[2] Departament de Genètica i de Microbiologia, Facultat de Biociències, Universitat Autònoma de Barcelona, 08193 Barcelona, Spain.

[3] Microbiology Section, Department of Genetics, Microbiology and Statistics, Faculty of Biology, University of Barcelona, 643 Diagonal Ave., 08028, Barcelona, Spain.

* Corresponding authors:

Dr. Esther Julián E-mail: esther.julian@uab.cat

Dr. Eduard Torrents E-mail: etorrents@ibecbarcelona.eu/eduard.torrents@ub.edu

Abstract

The incidence of infection by nontuberculous mycobacteria, mainly *Mycobacterium abscessus*, in patients with cystic fibrosis and other chronic pulmonary illnesses is increasing, translating into an acceleration in the decline of lung function. In most cases, *M. abscessus* coinfects with *Pseudomonas aeruginosa*, the most common pathogen in these chronic diseases. However, it is unknown how these two bacterial species interact when coinfecting. This study aims to explore the behavior of both species in three relevant pathogenic settings: dual-species biofilm development using a recently developed method to monitor individual species in dual-species biofilms; coinfection in bronchial epithelial cells using *in vitro* assays; and *in vivo* coinfection using the *Galleria mellonella* model. The results demonstrate the capability of both species to form stable mixed biofilms and to reciprocally inhibit single-biofilm progression. Coinfections in bronchial epithelial cells were correlated with significantly decreased cell viability, while in *G. mellonella,* coinfections induced lower survival rates than individual infections. Outstandingly, the analysis of the immune response triggered by each bacterium in bronchial epithelial cell assays and *G. mellonella* larvae revealed that *P. aeruginosa* induces the overexpression of proinflammatory and melanization cascade responses, respectively. In contrast, *M. abscessus* and *P. aeruginosa* coinfection significantly inhibited the immune response in both models, resulting in worse consequences for the host than those generated by single *P. aeruginosa* infection. Overall, the presence of *M. abscessus* produces a decline in the immune responses that worsens the infection and compromises the host.

Importance

The appearance of bacterial infections in the respiratory tract of patients with chronic respiratory diseases suppose a serious and difficult to treat health problem. This complication is exacerbated by the increase resistance against antibiotics generated by pathogenic microorganisms. The most common and virulent pathogenic bacteria reported in the respiratory airway is *Pseudomonas aeruginosa*. It is a Gram-negative, ubiquitous, and intrinsic resistant to antibiotics bacteria. However, the incidence of a rapidly growing, multi-drug resistant mycobacteria; *Mycobacterium abscessus*, is growing worldwide. The pulmonary coinfection by both pathogens is directly related with higher rates of morbidity and mortality of patients. The significance of our research is characterizing the behavior of these two pathogens when they coinfects together, exploring the immune response triggered by the host and its impact in the survival. The purpose is enhancing the limited understanding we have of this clinically relevant coinfection to favor the development of new effective treatments.

Keywords: dual-species biofilm, *Galleria mellonella*, nontuberculous mycobacteria, pulmonary epithelia.

59 **Introduction**

60 Cystic fibrosis (CF) is an autosomal recessive inherited condition caused by the presence of mutations in
61 the gene encoding the cystic fibrosis transmembrane conductance regulator (CFTR) protein (1). This
62 protein acts as a transporter channel that conducts chloride ions (Cl^-) across epithelial cell membranes to
63 maintain the balance of salt and water on many surfaces in the body and is especially relevant in the
64 respiratory system airways (2). A malfunction in CFTR protein prevents proper hydration of the cellular
65 surface, which leads to the loss of the mucus covering the cells, becoming thick and sticky (3). These
66 characteristics of the mucus in CF patients hinder the primary innate defense mechanism of the lung,
67 mucociliary clearance (4), leading to an increased risk of infections from different pathogens, especially
68 *Pseudomonas aeruginosa*, *Staphylococcus aureus*, *Burkholderia spp.* and nontuberculous *Mycobacterium*
69 *spp.* (NTM), which are associated with a high risk of pulmonary compromise and lead to chronic
70 infections (5). In fact, lung tract infections in CF patients are complex and polymicrobial, capable of
71 developing intermicrobial and host–pathogen interactions impacting clinically relevant features such as
72 virulence, persistent colonization of the airways, and antimicrobial recalcitrance (6, 7). Although CF
73 polymicrobial infections are highly individualized in each patient, *S. aureus* and *P. aeruginosa* dominate
74 in children and adult microbial communities, respectively. In this sense, the coinfection by these two
75 dominant pathogens or one of them with other species negatively affect respiratory function compared to
76 single infections (7).

77 *P. aeruginosa* is a ubiquitous gram-negative opportunistic pathogen that is metabolically flexible and
78 considered the most relevant bacterium associated with CF due to its high prevalence and pathogenesis.
79 Due to its ability to adapt to the CF pulmonary environment, *P. aeruginosa* is also the primary pathogen
80 present in advanced CF lung disease (8). *P. aeruginosa* PAO1 is the reference laboratory strain for
81 research and PAET1 strain is a clinical isolate from a cystic fibrosis chronically infected patient. *P.*
82 *aeruginosa* develops biofilms on the thick and dehydrated mucoid surface, which represents a difficult
83 barrier to antibiotic penetration and to host innate immune effectors, in CF (9). These biofilms cause
84 chronic infections through higher antibiotic tolerance, resistance to phagocytosis, and immune-mediated
85 chronic inflammation (10). Furthermore, biofilms are usually polymicrobial and are related to an
86 exacerbated inflammatory immune response that seriously compromises respiratory function, producing
87 the most extensive lung lesions (11).

88 A significant increase in the incidence of infections caused by NTM in CF patients has been recently
89 reported (12, 13), with fast-growing *Mycobacterium abscessus* being the most prominent and worrisome
90 pathogen of this genus (14). *M. abscessus* infections are associated with an increase in morbidity and
91 mortality due to the long duration of treatment related to significant adverse effects, its multiresistance to
92 antimicrobials, and consequently, the low success rate in its elimination from the respiratory tract (15).
93 Another relevant element in *M. abscessus* pathogenicity is its ability to modify its cell wall, which allows
94 the identification of two different morphotypes in this species: smooth (S), which contains abundant

95 glycopeptidolipids (GPLs) in the outer layer, and rough (R), which is devoid of GPLs (16). Similar to *P.*
96 *aeruginosa*, *M. abscessus* also has a biofilm-forming capacity, making treatment even more difficult.
97 Remarkably, 58-78% of patients with *M. abscessus* infection are also infected by *P. aeruginosa* (17). The
98 colonization of the lung epithelium begins with S morphotypes, which progressively switch to R mutants,
99 giving a more aggressive, invasive pulmonary infection (18). In this sense, biofilms developed by each
100 morphotype of *M. abscessus* present different mechanical properties, with R biofilms having higher
101 rigidity than S biofilms. Interestingly, *M. abscessus* R/S biofilms present more resistance to mechanical
102 forms of clearance from the lung than *P. aeruginosa* biofilms (19). Furthermore, *M. abscessus* biofilm
103 bacilli change the mycolic acid proportions and produce a lipid-relevant extracellular matrix with other
104 components, such as carbohydrates, proteins, or extracellular DNA (20).
105 Coinfections of *P. aeruginosa* and *M. abscessus* in CF have become clinically more relevant over the last
106 two decades; the incidence of NTM infections among CF patients has risen from 3.3% to 22.6%, resulting
107 in an increase in morbidity and mortality (16). In 16% to 68% of NTM-positive sputum cultures, the *M.*
108 *abscessus* complex is present, and its prevalence is increasing (12). Furthermore, the presence of *M.*
109 *abscessus* lung disease has been considered a strong relative contraindication to lung transplantation (21),
110 which can extend and improve the quality of life in properly CF patients, increasing their mean life
111 expectancy by 7.4 years (22).
112 Despite the challenges stated above, studies focused on the interaction between both species are scarce. It
113 is therefore crucial to further elucidate and characterize the *P. aeruginosa*-*M. abscessus* coinfections. For
114 this reason, the objective of the present study is to unravel the interaction mechanisms between both
115 bacteria, focusing on relevant aspects of pathogenicity: dual-species biofilm development using recently
116 developed coculture techniques, including S and R *M. abscessus* morphotypes, and the viability outcome
117 and the analysis of the triggered immune response by each species in individual and coinfection
118 experiments using *in vitro* and *in vivo* models. A better understanding of the behavior between *P.*
119 *aeruginosa* and *M. abscessus* would provide us with tools to develop efficient treatment strategies against
120 these pathogens in CF patients.
121
122 **Results**
123 ***M. abscessus reduces the progression of P. aeruginosa biofilms in vitro***
124 *In vitro* biofilm development assays (see Material and Methods) showed that the addition of *M. abscessus*
125 R or S to mature *P. aeruginosa* biofilms limits their growth capacity (**Figure 1A**). This inhibitory effect
126 was observed for both strains of *P. aeruginosa* PAO1 and PAET1 biofilms. Specifically, the presence of
127 *M. abscessus* (R and S) resulted in a growth reduction of approximately 20% for PAO1 and 30% for
128 PAET1 biofilms (**Figure 1A**) compared with the nontreated *P. aeruginosa* biofilms (represented as 100%
129 growth). Nevertheless, the highest rate of growth inhibition was reported with *M. abscessus* S at 10^4
130 cfus/well, with approximately 40% PAO1 biofilm reduction. The addition of heat-killed *M. abscessus* or
131 bacterial culture supernatants had no inhibitory effect on the growth of *P. aeruginosa* mature biofilms

132 (**Figure 1A**). Similarly, the use of *E. coli* (gram-negative) or *B. thuringiensis* (gram-positive) did not have
133 a growth-limiting effect on *P. aeruginosa* biofilms and even, in the case of heat-killed *E. coli* and
134 supernatant from *E. coli* cultures, induced *P. aeruginosa* PAO1 biofilm growth (**Figure 1A**).
135 When *P. aeruginosa* strains were cocultured simultaneously with all bacteria tested, the results were
136 comparable with the previous assay results but with slight inhibition percentage changes in some cases
137 (**Figure 1B**). *P. aeruginosa* PAO1 cocultured with the *M. abscessus* R morphotype showed a 30%
138 reduction in PAO1 biofilm compared to the control, while with the S morphotype, the reduction in PAO1
139 biofilm was only approximately 20%. In *P. aeruginosa* PAET1 cocultures, the results using *M. abscessus*
140 R or S were quite similar, with an approximately 30% decrease in PAET1 biofilm compared to the
141 control (growth of *P. aeruginosa* alone) (**Figure 1B**). As previously shown in Figure 1A, the addition of
142 *E. coli* and *B. thuringiensis* and the use of heat-killed cultures or supernatants did not have an inhibitory
143 effect on the *P aeruginosa* PAO1 and PAET1 biofilms (**Figure 1B**). Also, it was observed that PAET1
144 biofilms progression was highly inhibited in coculture with *M. abscessus* (R and S) than those of PAO1 in
145 all the biofilm assays tested.
146 After observation of a clear *P. aeruginosa* biofilm reduction with the addition of *M. abscessus*, either
147 added in a mature biofilm or when simultaneously grown in a dual-species biofilm, the structure and
148 composition of coculture biofilms were analyzed by confocal microscopy. The images showed that after
149 24 h of coculture, *M. abscessus* was established in a *P. aeruginosa* mature biofilm, demonstrating the
150 capacity to settle and simultaneously grow under these conditions (**Figure 1C**). The presence of *P.*
151 *aeruginosa* cells (in blue) was clearly higher, but *M. abscessus* bacilli (in green) were clearly observed in
152 both *P. aeruginosa* PAO1- and PAET1-formed biofilms and quantitatively represented between 25 to
153 35% of the sample, as shown in the pixel color quantification graph (**Figure 1C**). This result
154 demonstrates that both species can survive and coexist in a dual-species biofilm. Apparently, the presence
155 of both morphotypes R and S of *M. abscessus* is higher in the *P. aeruginosa* PAET1 biofilm than in
156 PAO1, consistent with the results obtained in **Figure 1A,** where growth inhibition was higher for the
157 PAET1 strain using the same experimental conditions than for the PAO strain. Regarding the structure of
158 the biofilm, it was observed through orthogonal projections that *P. aeruginosa* and *M. abscessus* were
159 heterogeneously distributed along the biofilm without predominantly occupying any specific area
160 (**Supplementary Figure 2**).
161 In view of the results obtained, a possible direct inhibitory effect between *P. aeruginosa* PAO1/PAET1
162 growth and some molecules released by *M. abscessus* R and S, *E. coli* or *B. thuringiensis* was tested. For
163 this purpose, all bacteria were cultivated on agar plates in close streaks where no inhibitory effects were
164 observed on the growth of any bacteria by the presence of the others (**Supplementary Figure 5A)**.
165 Kinetic curves of *P. aeruginosa* PAO1 and PAET1 planktonic growth were also generated by
166 cocultivation with culture supernatants of the other bacteria, and similar to the solid agar cultures, no
167 significant inhibitory effect on the growth of *Pseudomonas* was reported (**Supplementary Figure 5B and**
168 **5C)**.

169

170 ***P. aeruginosa reduces the development of M. abscessus biofilms***

171 Although infection by *M. abscessus* in CF patients generally occurs in patients previously infected with *P.*
172 *aeruginosa*, we aimed to study the effect of *P. aeruginosa* on well-developed biofilms of *M. abscessus*.
173 Over a mature *M. abscessus* biofilm (120 h old), the addition of *P. aeruginosa* is directly related to a clear
174 reduction in the development of the *Mycobacterium* biofilm (both for R and S biofilms) (**Figure 2A**),
175 similar to the opposite case (**Figure 1A**). In detail, biofilm inhibition was notably higher in the *M.*
176 *abscessus* S morphotype than in the R morphotype for all the conditions tested. Additionally, *P.*
177 *aeruginosa* PAO1 induced a higher growth inhibitory effect in both *M. abscessus* biofilm morphotypes
178 than the *P. aeruginosa* PAET1 strain. These results obtained by GFP quantification were corroborated
179 using confocal microscopy (**Figure 2B**). The images show that after treatment of an *M. abscessus* biofilm
180 with *P. aeruginosa,* both bacteria form a combined biofilm in which *P. aeruginosa* expands rapidly due to
181 its competitive advantage in growth rate. The detection of mycobacteria by GFP in coculture conditions
182 was reduced compared with that of the control biofilms (without *P. aeruginosa*), and a lower presence of
183 *M. abscessus* was also detected in the S morphotype compared to the R in combination with both *P.*
184 *aeruginosa* PAO1 and PAET1 (**Figure 2B**).

185

186 ***Coinfection of M. abscessus and P. aeruginosa in bronchial epithelial cells reduces the viability and***
187 ***immune response triggered with respect to single P. aeruginosa infection***

188 For determination of the effect of bacterial coinfection in the CF context, CFBE41o- (homozygous for the
189 ΔF508 CFTR mutation) and 16HBE14o- (usually differentiated bronchial epithelial cells) bronchial
190 epithelial cells were infected with *P. aeruginosa*, *M. abscessus, B. thuringiensis* or combinations of
191 bacteria. The results showed a reduction in viability of approximately 10-30% in infected cells with
192 respect to uninfected cells in all cases (**Figure 3A**). Remarkably, while single infection with *M. abscessus*
193 variants or *B. thuringiensis* reduced viability up to 5-15% in both cell lines, when cells were coinfected
194 with either of the two *P. aeruginosa* strains, viability was significantly diminished with respect to single
195 infection (Figure 3A). In all cases, the viability levels of coinfected cells were similar to those obtained
196 with single infection of *P. aeruginosa* strains, with the exception of the *P. aeruginosa* strains PAO1 and
197 PAET1, and *M. abscessus* R coinfected cells, in which lower viability was obtained (Figure 3A). No
198 differences were obtained between cell lines, indicating that the inhibitory effect of the bacteria is not
199 dependent on the epithelial characteristics.

200 Differences were observed for each culture condition when IL-6 and IL-8 production was analyzed. When
201 cytokine production was analyzed in cell culture supernatants, *P. aeruginosa*-infected cell lines showed
202 the highest amount, indicating an elevated inflammatory response (**Figure 3B**). Single infections with *M.*
203 *abscessus* R and S and *B. thuringiensis* showed different stimulatory capabilities, while *M. abscessus* S
204 did not induce the production of cytokines, *B. thuringiensis* triggered only IL-8 production in both cell

205 lines, and *M. abscessus* R triggered IL-6 production in both cell lines and IL-8 only in the control cell line
206 (**Figure 3B**).
207 The most relevant result was observed in cells coinfected with both bacteria. *M. abscessus* coinfection
208 was able to inhibit the higher production that was reported by *P. aeruginosa* single-infected cells, and the
209 release of IL-6 and IL-8 was reduced to levels similar to those triggered by *M. abscessus* single infection
210 (**Figure 3B**). *M. abscessus* S and *P. aeruginosa* (both strains) coinfection reduced the production of
211 cytokines to levels similar to those in the control cells. Strikingly, this effect observed with *M. abscessus*
212 was not observed when *B. thuringiensis* was coinfecting with *P. aeruginosa*, triggering cytokine levels
213 similar to those produced by *P. aeruginosa* single infections (Figure 3B). No differences were observed
214 between cell lines.
215
216 ***M. abscessus and P. aeruginosa coinfection accelerates G. mellonella larval death***
217 The *G. mellonella* larvae *in vivo* model presents an immune system broadly similar to mammalian innate
218 immunity being useful for the characterization of microbial infections and host-pathogen interactions.
219 Infection by both *P. aeruginosa* PAO1 and PAET1 strains is lethal for *G. mellonella* larvae. However, *M.*
220 *abscessus* infections need prolonged times (up to 144 h) and high concentrations (10^6 cfus/larva) to
221 become lethal (see Materials and Methods section and **Supplementary Figure 3**). Coinfection with *M.*
222 *abscessus* R and S but not with *B. thuringiensis* accelerated the survival decline in the larvae in both
223 strains and all concentrations tested compared to the infections of *P. aeruginosa* strains alone (**Figure 4**).
224 This overtaking lethality was clearly observed, being significant for all *M. abscesssus* and *P. aeruginosa*
225 coinfection combinations tested and specially in the of PAO1 plus *M. abscessus* R coinfection. We
226 corroborated that the causal agent of larval death was the presence of *P. aeruginosa* PAO1 or PAET1 in
227 the larvae by detecting the luminescence in their interior trough *lux* detection in a luminescence analysis
228 (**Supplementary Figure 4**). As Figure 4 shows, *B. thuringiensis* coinfection did not modify larval
229 survival rates.
230
231 ***M. abscessus and P. aeruginosa coinfection restricts the immune response of G. mellonella larvae***
232 *G. mellonella* larvae produce several antimicrobial peptides (AMPs) and enzymes in response to
233 infection. The results of immune-relevant *G. mellonella* gene expression showed a significant decrease in
234 the transcriptional induction for several genes tested, comparing *P. aeruginosa* individual infections with
235 different coinfection conditions (**Figure 5**). For gloverin, cecropin D, transferrin, moricin, lysozyme,
236 insect metalloproteinase inhibitor (IMPI) and nitric oxide synthase (NOS) gene expression, a comparable
237 trend was observed between all the infections assayed. Briefly, high induction of gene expression in
238 PAO1- and PAET1-infected larvae was observed, with lower induction of gene expression in larvae
239 coinfected with *B. thuringiensis* and *P. aeruginosa* strains and notably lower gene expression in the case
240 of larvae infected with both *M. abscessus* R and S alone and coinfected with *P. aeruginosa* (**Figure 5**).
241 These data indicated that the presence of *M. abscessus* generated a decrease in gene expression compared

242 with the infection of single *P. aeruginosa* strains, leaving the induction of larvae coinfected by both
243 bacteria at the levels established by the mycobacteria alone.
244 Apolipophorin III (Apo III) and glutathione S-transferase (GST) resulted in a similar trend, with no
245 significant differences detected compared to the control (PBS-infected larvae) in any conditions except
246 for the *P. aeruginosa* PAO1-infected larvae, which showed evident repression of both genes. NADPH
247 oxidase (NOX4) gene expression was the only one that did not show significant differences in any of the
248 infections tested. In the case of hemolin, increased gene expression was observed in *M. abscessus*-
249 infected larvae, much higher than in the other studied genes and higher than in *B. thuringiensis* infection
250 conditions. This result contradicts the rest of the immuno-relevant gene tendencies. Hemolin acts as an
251 opsonin and mediates the interaction between microorganisms and hemocytes, stimulating phagocytosis.
252 In this work, we have also shown that *M. abscessus* R and S could be phagocytosed by *G. mellonella*
253 hemocytes (**Supplementary Figure 6A**) and progressively eliminated from the larva (**Supplementary**
254 **Figure 6B**), which would explain this contradictory result compared to the rest of the genes.
255
256 **Discussion**
257 Infections of the respiratory tract epithelium are the leading cause of morbidity and mortality in CF
258 patients. *P. aeruginosa* is the most relevant pathogen due to its robust virulence systems and biofilm-
259 forming capacity, which trigger increased tolerance to antibiotics and resist phagocytosis (9, 23).
260 Although *P. aeruginosa* is the most common and prevalent pathogen in CF patients, other
261 microorganisms, such as *S. aureus*, *Haemophilus influenzae*, *Stenotrophomonas maltophilia*, NTM, and
262 *Burkholderia* species, are presently forming a polymicrobial environment. Within the NTM group, *M.*
263 *abscessus* is the most relevant pathogen in CF patients since its multidrug-resistant and biofilm formation
264 capabilities (20, 24) widely increase antibiotic resistance and prevalence. In this work, the relationship
265 between *P. aeruginosa* PAO1 (laboratory strain)/PAET1 (clinical isolate) and *M. abscessus* R/S
266 morphotypes was studied for the first time in different contexts of critical interest: biofilm development,
267 bronchial epithelial cell *in vitro* cultures and *G. mellonella* larvae *in vivo* infection.
268 Regarding biofilm development, the results indicate a decrease in the progression of *P. aeruginosa*
269 biofilms when live *M. abscessus* R and S were introduced, independent of whether the biofilm was
270 already well established (mature biofilm) or in coculture biofilm growth. Inhibition of *Pseudomonas*
271 biofilm development by cocultivation with other pathogens commonly found in the lungs of CF patients,
272 such as *Aspergillus,* or potential probiotics, such as lactobacilli, has already been reported (25, 26).
273 Nevertheless, no inhibitory effect has been reported previously for mycobacteria. This inhibition could be
274 related to the capacity of *M. abscessus* to inactivate quorum sensing quinolone signals from *P. aeruginosa*
275 (27). In addition, the results showed that both species coexist in dual-species biofilms, with *P. aeruginosa*
276 being the dominant species, most likely related to its competitive advantage in terms of growth since *M.*
277 *abscessus* has a division time of 4 to 5 h, while *P. aeruginosa* has a division time of only 25 to 35 min
278 (28, 29). Conversely, biofilms of *M. abscessus* are also inhibited by the presence of *P. aeruginosa,* which

279 outcompetes mycobacteria, as previously reported in biofilm coculture experiments (30). The mechanism
280 responsible of this inhibition remain still unknown and *P. aeruginosa* interbacterial competition secretion
281 systems and quorum sensing seem to be not involved (31). Distinctly, the growth of S morphotype
282 biofilms, despite forming biofilm more easily by the abundance of GPLs in its cell wall (32), is inhibited
283 more by the presence of *P. aeruginosa* than R morphotype biofilms, which could be related to the
284 aggregative phenotype that confers higher resistance to antibiotics as well as structural rigidity (33).
285 These results indicate a decrease in both species biofilm progression when coculturing. It can be
286 hypothesized that this effect could not be due to direct inhibition but rather a consequence of the
287 combined growth of both species sharing the same space and competing for the same culture medium.
288 This hypothesis is partly supported by the lack of direct inhibition observed in agar plate cultures using
289 *M. abscessus* R and S cultured close to *P. aeruginosa* PAO1 and PAET1 or in planktonic growth kinetics
290 curves of *P. aeruginosa* PAO1 and PAET1 in combination with culture supernatants of the rest of
291 bacteria, in which no significant effect on the growth of *P. aeruginosa* was highlighted (**see**
292 **Supplementary Figure 5**). Also, the limitation in the progression of the *P. aeruginosa* PAO1 biofilm
293 was observed in co-culture with a non-pathogenic environmental mycobacteria such as *Mycobacterium*
294 *brumae* (data not shown). It has been demonstrated that in dual-species biofilms, antibiotic treatment to
295 eliminate *P. aeruginosa* supposes a competitive advantage for *M. abscessus* development (17). In any
296 case, *M. abscessus* establishes itself effectively and, despite its difference in growth rate, prevails in dual-
297 species biofilms, demonstrating its resistance and survival capabilities (34).
298 Regarding the effect of coinfection on bronchial epithelial cell viability *in vitro*, it has been shown that
299 coinfection results in higher mortality compared to individual *M. abscessus* and *B. thuringiensis*
300 infections, as expected. However, as previously reported (35), the viability of the cell lines tested,
301 CFBE41o- and 16HBE14o-, was not excessively compromised, being approximately 80% of the control
302 in all tested conditions. *M. abscessus* and *P. aeruginosa* coinfections correlate with an elevated
303 pulmonary function decline and worse disease severity (36, 37); therefore, lower viability of the epithelial
304 cells could be involved in these complications. The inflammatory response triggered by epithelial cells
305 shows a clearly exacerbated production of proinflammatory cytokines, IL-6 and IL-8, in response to
306 PAO1 and PAET1 single infections (see Figure 3). This immune response against *P. aeruginosa* is
307 harmful to patients, as excessive inflammation is responsible for most of the morbidity and mortality in
308 CF (38–40). Surprisingly, coinfection of *M. abscessus* and *P. aeruginosa* with epithelial cells showed an
309 evident inhibition of the proinflammatory response promoted by the mycobacteria since single *M.*
310 *abscessus*-infected cells presented similar production levels as the coinfected cells, being especially
311 prominent in the case of *M. abscessus* S. In general, microorganisms that occupy the airways together
312 with *P. aeruginosa* also induce a proinflammatory response, as in the case of *B. cenocepacia, H.*
313 *influenzae, S. aureus* and *Candida spp.* among others (41, 42). A comparable inflammatory reduction
314 effect to that observed for *M. abscessus* in our results has only been demonstrated in *P. aeruginosa*
315 coinfections with *Prevotella spp*. an anaerobic gram-negative bacterium belonging to the respiratory tract

316 microbiota (43). In the case of *M. abscessus*, previous works demonstrated that bronchial epithelial cells
317 generate a hyporesponsive response since *M. abscessus* S fail to elicit a Toll-like receptor 2 (TLR2)
318 response and only a precise cell fraction from R morphotype exhibits TLR2 stimulating activity (44),
319 which is necessary for the activation of the signaling cascade that triggers the secretion of the cytokines
320 IL-6 and IL-8 (45). This lack of immune response activation observed is particularly high in the case of
321 the S morphotype (as supported by our results) since the presence of GPL in its cell wall masks other
322 molecules that would activate TLR2 signaling (46). In most cases, this factor also explains why initial *M.*
323 *abscessus* colonization of lung airways occurs with an S morphotype strain. In the CF context, a
324 beneficial immune response consists of the capacity to activate an inflammatory response to manage
325 infection but to avoid an exuberant response that can be harmful (47). In the present study, cocultures of
326 *M. abscessus* and *P. aeruginosa* showed less inflammatory activation and the highest loss of viability
327 among infected cells, while cocultures of *B. thuringiensis* and *P. aeruginosa* showed a high inflammatory
328 response, leading to a high loss of viability. These results could indicate that an excessive
329 proinflammatory response and significant immune inhibition could be equally harmful to infected lung
330 epithelial cells.
331 The results of the *in vitro* cultures were corroborated by infections in the *G. mellonella* larva model, in
332 which an increased lethality was observed in coinfection conditions with respect to the single *P.*
333 *aeruginosa* infection. *G. mellonella* is highly susceptible to *P. aeruginosa* infections since 100% larval
334 lethality is reached in less than 24 h with few inoculated bacteria (10-30 CFU) (48, 49) although there are
335 important variations in pathogenicity and lethality between strains commonly used in research (PAO1 in
336 this study) and clinical isolates (PAET1 in this study) (35, 50). However, *M. abscessus,* despite being
337 pathogenic for larvae, requires much higher doses and prolonged infection times than *P. aeruginosa* to be
338 equally lethal ((51, 52), and **Supplementary Figure 3**). In addition, in agreement with our *in vitro* results,
339 the immune response of *G. mellonella* larvae was clearly inhibited under coinfection conditions (Figure
340 5). The gene expression of most proteins and enzymes related to larval immunity showed a significant
341 decrease compared with that of *P. aeruginosa* strain single infections (53). In detail, relevant AMPs
342 involved in antimicrobial activity, such as gloverin, cecropin D and moricin, were clearly inhibited in
343 coinfection conditions. All of them act against the bacterial cell wall by interacting with LPS and other
344 components, especially affecting the outer membrane of gram-negative bacteria (54–56); specifically,
345 moricin is capable of forming pores in gram-positive and gram-negative cell walls (57). Under
346 coinfection conditions, insect metalloproteinase inhibitor (IMPI) expression was also inhibited; this
347 peptide has only been described thus far in *G. mellonella* (58) and inhibits the activity of proteases
348 secreted by invading microorganisms (59). In this sense, it is well known that *P. aeruginosa* produces
349 various proteases as virulence factors (60); thus, high levels of IMPI would potentially slow the
350 progression of *P. aeruginosa* infection. Furthermore, IMPI inhibits the activation of phenoloxidase, the
351 activator enzyme of the melanization cascade (61). The produced melanin is deposited around the
352 pathogenic microorganism, limiting its ability to damage the larva, but in parallel to melanin production,

353 dangerous substances and reactive substances are also produced, resulting in tissue damage and cell
354 death, which could be self-defeating for the host (62). Additionally, the expression levels of immune-
355 relevant proteins and enzymes, transferrin, lysozyme and nitric oxide synthetase (NOS), are notably
356 inhibited when *M. abscessus* and *P. aeruginosa* are infecting simultaneously. Lysozyme is a cationic
357 peptide with muramidase activity (63) that degrades peptidoglycan, making it more effective against
358 gram-positive bacteria and, similar to IMPI, preventing an excessive melanization response (64).
359 Transferrin mediates nutritional immunity by sequestering iron from invading pathogens, limiting their
360 ability to grow and develop (65). *P. aeruginosa* needs substantial amounts of iron to grow and produces
361 two siderophores to take up this metal (66), so high levels of transferrin in the hemolymph are beneficial
362 to host survival. The production of nitric oxide by NOS under infection conditions is increased, although
363 its role in immunity is not entirely clear (67), although it is hypothesized that it is transformed into
364 reactive nitrogen species that are highly toxic to bacteria but equally toxic to host cells (68). Moreover,
365 the expression levels of glutathione S-transferase (GST) and apolipophorin III (Apo III) are clearly
366 repressed only in *P. aeruginosa* PAO1-infected larvae, while they remain unchanged in the other
367 conditions, including *P. aeruginosa* PAET1, which indicates differences in the immune response against
368 both *P. aeruginosa* strains. GST is a detoxification enzyme that protects the host from oxidative stress
369 (69). To reduce pathogen progression, larvae induce a prophenoloxidase response, which triggers the
370 production of reactive oxygen species to damage bacteria, although it also affects host cells (70);
371 therefore, it would make sense to inhibit antioxidative enzymes, such as GST, under severe infections.
372 Apo III is a lipid transport protein with relevant immune effects since it mediates hemocyte adhesion,
373 phagocytosis and nodule formation (71). *P. aeruginosa* serine protease IV was shown to degrade Apo III
374 (72, 73); however, the results of our study show that Apo III levels are also reduced at the transcriptional
375 level. In addition to the protease activity of *P. aeruginosa*, low levels of Apo III in hemolymph could be
376 reinforced by a repressive effect on its synthesis. NADPH oxidase (NOX4) is the only enzyme that did
377 not present significant differences between infected and uninfected larvae. This enzyme produces
378 superoxide and reactive oxygen species in response to infection, suggesting that it is not overexpressed
379 under the infection conditions tested in this study due to the production of these toxic agents by the
380 prophenoloxidase pathway (74), which is highly induced, as previously mentioned.
381 The repressive effect of *M. abscessus* R and S, together with *P. aeruginosa* PAO1 and PAET1
382 coinfections, was observed in most of the genes evaluated. However, as the only exception, an induction
383 of transcriptional expression of the hemolin gene in *M. abscessus*-infected larvae (especially the R
384 variant) was shown. Hemolin is an immunoglobulin-like protein with no direct antibacterial properties
385 associated with hemocytes in the pathogen recognition process. This protein functions as an opsonin that
386 mediates between bacteria and hemocytes, stimulating the phagocytosis process. Surprisingly, this study
387 shows the phagocytic capacity of *G. mellonella* hemocytes against *M. abscessus* bacilli (**Supplementary**
388 **Figure 6**), which could be directly related to this singular overexpression detected in mycobacterium-
389 infected larvae.

390 Overall, the transcriptional expression levels of the different genes investigated show high induction
391 levels in the single infections of *P. aeruginosa*, although slight differences between PAO1 and PAET1
392 strains are marked, showing different responses. In *M. abscessus*-infected larvae, expression levels are
393 notably lower and remain at similar levels in both single and coinfections. This repression of the larvae
394 innate immune response could be attributed to the extensive phagocytosis of mycobacteria by hemocytes,
395 which may proliferate and thereby limit the antibacterial activity of these cells, consequently hindering a
396 robust specific response against *P. aeruginosa*. Additionally, prior studies have highlighted *M. abscessus*
397 specific affinity for colonizing and infecting the fat body tissue of *G. mellonella* larvae (75), which serves
398 as the primary source of antimicrobial peptides, enzymes, and antibacterial proteins secreted into the
399 hemolymph (59). Hence, the presence of *M. abscessus* in the fat body could account for the diminished
400 production of these molecules that correlates with the acceleration in lethality in the coinfection
401 conditions. Notably, larvae infected with *B. thuringiensis* follow trends similar to those of individual *P.*
402 *aeruginosa* infections, although interestingly showing lower levels than these.
403 The observed results in the immune response triggered by bronchial epithelial cells and *G. mellonella*
404 larvae are compatible with the decreased response degree under coinfection and contrary to the
405 overexpressed response under *P. aeruginosa* single infections. The hyperinflammatory response produced
406 in the airways by *P. aeruginosa* infection is well described in patients (76), producing more severe
407 respiratory malfunction usually treated with corticosteroids (77). In the case of *M. abscessus*, it has been
408 shown in a murine model of CF that the proinflammatory response produced is higher in the R
409 morphotype than in the S morphotype (78), in accordance with the IL-6 and IL-8 differences detected in
410 our study. The immune repression shown in the coinfections of *M. abscessus* and *P. aeruginosa* is
411 described for the first time in this work. A disproportionate immune response is dangerous for the host
412 since excess inflammation and the production of toxic compounds for bacteria and the host trigger a
413 decline in survival. However, the weak immune response observed in coinfections with *M. abscessus* is
414 even worse since the bacteria can spread unrestrictedly, triggering lethality at shorter times, as shown in
415 the results of the *in vivo* survival and *in vitro* viability assays in this work. Taking this study as a starting
416 point, and in order to generalize the results, it will be necessary to explore whether the results obtained
417 are replicable using other strains of *P. aeruginosa* and *M. abscessus* beyond those employed in this study,
418 particularly with clinical relevance, which allow establishing a clear pattern of interaction between both
419 species when they are coinfecting simultaneously.
420

421 **Materials and Methods**

422 ***Bacterial strains and culture conditions.***

423 Two different *P. aeruginosa* strains were used: PAO1 (ATCC 15692) as a reference laboratory strain and
424 PAET1, a clinical isolate from a chronic CF-infected patient (79). Both strains were transformed with a
425 plasmid (pETS130lux) expressing a constitutive bacterial luciferase gene cassette (*lux*) as a
426 bioluminescent bioreporter system (80). Both *P. aeruginosa* strains were grown in Luria-Bertani (LB,

427 Sharlab, Barcelona, Spain) agar with 50 µg/ml gentamycin (Gm) for PAO1 and 300 µg/ml carbenicillin
428 (Cb) for PAET1 as a selection marker. For biofilm formation assays, *P. aeruginosa* was grown in tryptic
429 soy broth (TSB, Sharlab) without antibiotics. *Bacillus thuringiensis* (ATCC 10792) was cultured in
430 tryptic soy agar (TSA, Sharlab) or TSB, and *Escherichia coli* MG1655 (ATCC 700926) was grown in LB
431 (agar and broth). The *M. abscessus* DSMZ 44196 (ATCC 19977) original smooth (S) morphotype and the
432 rough (R) variant, a natural mutant of the wild-type strain previously obtained (81), were grown on TSB
433 with agitation and 0.5 mm diameter glass beads (DDBiolab, Barcelona, Spain) to prevent cell aggregation
434 and on TSA agar for colony forming unit (CFU) counting. As previously reported, both variants of *M.*
435 *abscessus* were transformed with the plasmid pETS218 (82). For further detail regarding the strains used,
436 see **Supplementary Table S1**.
437
438 ***DNA manipulation and plasmid construction***
439 Molecular biology enzymes and kits were purchased from Thermo Fisher Scientific (Madrid, Spain) and
440 used according to the manufacturer's instructions. DNA amplification was performed by PCR using
441 DreamTaq MasterMix (2X) or High-Fidelity PCR Enzyme Mix (Thermo Fisher Scientific). The primers
442 used are listed in **Supplementary Table S2**. Plasmid pETS218 was constructed by cloning the promoter
443 region of the class Ib ribonucleotide reductase (encoded by the *nrdHIE* genes) from *M. brumae* (GenBank
444 assembly accession: GCA_900073015.1). All other recombinant DNA manipulations were performed
445 using standard procedures (83). For construction of mycobacterial *nrdH* transcriptional GFP fusions, a
446 537 bp long fragment encompassing the *nrdH* promoter region was amplified by PCR using the primer
447 pair MbruPnrdHIE-For-MbruPnrdHIE-Rev and *M. brumae* genomic DNA; the obtained DNA fragment
448 was cloned into pJET1.2 and transformed into *E. coli* DH5α cells. *BamHI* and *Apa*I restriction enzymes
449 were used for fragment digestion and cloning into pFPV27 (84) to generate pETS218. The absence of
450 mutations introduced during cloning was verified via DNA sequencing. *M. abscessus* S and R
451 morphotypes were grown in TSA plus 50 µg/ml kanamycin (Kn) when they were transformed with
452 pETS218 as we previously described (82).
453
454 ***Biofilm progression inhibition quantification***
455 Biofilm quantifications were performed using a microtiter plate screening assay previously optimized,
456 validated and published in our group (85). Briefly, mature *P. aeruginosa* PAO1 and PAET1 biofilms (72
457 h growth) were cocultured with *B. thuringiensis*, *E. coli* and *M. abscessus* R and S for 24h further. For
458 this purpose, ON cultures of *B. thuringiensis* and *E. coli* were adjusted to an OD_{550} nm of 1 and
459 appropriately diluted to obtain the desired concentrations. *M. abscessus* R and S were grown for 3 days on
460 TSB cultures, and the concentrations of both live and heat-killed (121 °C for 21 min) cell suspensions
461 were determined by comparison to the MacFarland 1 (McF) turbidity standard. Bacterial culture
462 supernatants were also obtained by centrifugation of these cultures at 12,000 g. Serial dilutions of the
463 bacterial suspensions were plated to verify the accurate concentration in each experiment for all bacteria

464 tested. The level of lux expression (*P. aeruginosa* cells) in the biofilms was quantified using a Spark®
465 multimode microplate reader (Tecan, Männedorf, Switzerland). For simultaneous dual-species biofilm
466 formation experiments, *P. aeruginosa* PAO1 and PAET1 suspensions were mixed with the rest of
467 bacteria or supernatants and grown for 72 h.
468
469 ***M. abscessus biofilm formation and P. aeruginosa coexistence***
470 Three-day-old liquid cultures of *M. abscessus* R and S transformed with pETS218 plasmid were adjusted
471 to a concentration of $5x10^6$ cfu/ml and grown in TSB medium + 0.2% glucose in Costar® 96-Well Black
472 Polystyrene Plates (200 µl/well) (Corning) at 37 °C in saturation humidity conditions to allow
473 mycobacterial biofilm formation. After 120 h of incubation, 3 washes with PBS were carried out, and
474 suspensions of *P. aeruginosa* PAO1 and PAET1 cultures were added at an $OD_{550\ nm}$= 0.1 for an additional
475 72 h. Finally, the biofilms were homogenized in PBS and quantified by measuring the GFP and *lux*
476 expression associated with *M. abscessus* and PAO1/PAET1 growth, respectively, using a Spark®
477 multimode microplate reader.
478
479 ***Biofilm analysis through confocal microscopy***
480 The *P. aeruginosa* and mycobacterial biofilms developed in 96-well plates were collected, and bacteria
481 were stained with 4',6-diamidino-2-phenylindole (DAPI). *M. abscessus* R and S (transformed with
482 pETS218) bacilli were specifically detected by measuring their GFP expression. Representative images
483 were obtained in a Zeiss LSM 800 confocal laser scanning microscope (CSLM, Zeiss, Oberkochen,
484 Germany) using the 63×/1.4 oil objective with excitation wavelengths of 405 and 488 nm for DAPI and
485 GFP, respectively. Five representative Z-stack images were selected and analyzed for pixel color
486 quantification using the color histogram tool from Fiji-ImageJ software and Zen software (Zeiss).
487
488 ***Galleria mellonella maintenance and infection***
489 *G. mellonella* larvae were fed *at libitum* with an artificial diet as previously described (80). The larvae
490 were kept at 34 °C in a dark environment until they reached their optimum size (approximately 200 mg).
491 *G. mellonella* larvae were injected with 10 µl of bacterial suspension containing the desired concentration
492 through the top right proleg using a 25 µl Hamilton microsyringe (Hamilton, Reno, USA). In previous
493 experiments, lethal and innocuous doses of each bacterium were determined (**Supplementary Figure 3**).
494 Based on these results, the highest safe doses were selected: 10^4 CFU/larva for *M. abscessus* R and S and
495 10^5 CFU/larva for *B. thuringiensis* and *E. coli*. In the case of *P. aeruginosa*, even the lowest dose tested
496 (10 CFU/larva) was lethal. The virulence of the *P. aeruginosa* PAO1 strain was much higher than that of
497 PAET1; therefore, the PAET1 strain dose was adjusted to 10^4 CFU/larva, similar to 10 CFU/larva of
498 PAO1. Thirty larvae were infected with each condition, *E. coli*, *B. thuringiensis* and *M. abscessus* R/S,
499 and were then injected with the *P. aeruginosa* PAO1 or PAET1 strains. Additionally, larvae infected with
500 only each *P. aeruginosa* strain were used as controls for comparison purposes. Infected larvae were kept

501 at 37 °C to allow the development of infection for 14 h. At that time, five larvae were used to extract
502 RNA, and thirty were monitored for survival for 24 h.
503 For analysis of the phagocytosis of *M. abscessus* R and S by *G. mellonella* hemocytes and the
504 concentration of mycobacteria in the hemolymph (**Supplementary Figure 6**), the larvae were infected
505 with 10^4 CFU/larvae of each variant. For collection of hemolymph, larvae were placed on ice for 10 min.
506 Once anesthetized, the anal proleg was cut with a surgical blade, and the hemolymph was collected in a
507 1.5 ml Eppendorf tube. Hemolymph from 10 larvae was pooled and appropriately diluted and cultured on
508 TSA plates for mycobacterial CFU counts. The hemolymph from the other 10 larvae was centrifuged and
509 washed 3 times with PBS (5 min at 500 g at 4 °C). Precipitated hemocytes were resuspended in PBS and
510 stained with DAPI (blue) (4′,6-diamidino-2-phenylindole) to observe nuclei and with FM 4-64 (red) (N-3-
511 triethylammoniumpropyl-4-6-4-diethylamino phenyl hexatrienyl pyridinium dibromide) for dying
512 hemocyte vesicles and plasma membrane and observed under a confocal microscope (Zeiss LSM 800
513 confocal laser scanning microscope (CSLM)).
514
515 ***G. mellonella RNA extraction and immune-relevant gene expression analysis***
516 At 14 h post-infection, five larvae were placed on ice for 10 min. The larvae were homogenized using a
517 rotor-stator homogenizer (IKA, Staufen, Germany), and 30 mg of the homogenate was used for RNA
518 extraction following the GeneJET RNA Purification Kit instructions (Thermo Fisher Scientific). RNA
519 obtained was treated with 10x TURBO DNase (Life Technologies, Carlsbad, USA) for 1 h to eliminate
520 possible DNA contamination. DNA absence was verified by PCR amplification of the 18S rRNA
521 housekeeping gene using genomic DNA of *G. mellonella* as a positive control. RNA was quantified in an
522 M200 PRO microplate reader (Tecan). RNA to cDNA reverse-transcription was performed using Maxima
523 Reverse Transcriptase (Thermo Fisher Scientific) with Oligo (dT)18 primers (Thermo Fisher Scientific)
524 by following the manufacturer's instructions. The cDNA obtained was stored at -20 °C until use.
525 Quantitative real-time PCR (qRT-PCR) was performed using PowerUp™ SYBR™ Green Master Mix
526 (Applied Biosystems, Foster City, CA, USA) in a StepOnePlus™ Real-Time PCR System (Applied
527 Biosystems) according to the manufacturer's protocol. All qRT-PCRs used specific primers of *G.*
528 *mellonella* immune-relevant genes listed in **Supplementary Table 2**.
529
530 ***Bronchial epithelial cell line culture and infection***
531 Two human bronchial epithelial cell lines were used: CFBE41o-, isolated from a CF patient homozygous
532 for the ΔF508 CFTR mutation, and 16HBE14o-, isolated from a cardiopulmonary patient with
533 overexpression of CFTR (35). Cells were maintained in Dulbecco's modified Eagle's medium: nutrient
534 mixture F12 (DMEM/F12; Thermo Fisher Scientific) with 10% (v/v) decomplemented fetal bovine serum
535 (dFBS) (Gibco, Paisley, UK) and 1% (v/v) penicillin–streptomycin (Thermo Fisher Scientific). Cells were
536 maintained in a humidified incubator at 37 °C and 5% (v/v) CO_2 (ICOmed, Memmert). For infection
537 experiments, cells ($5x10^4$ cell/well) were incubated in 96-well plates (Corning) using antibiotic- and

538 serum-free medium for 3 h to allow cell adhesion. Subsequently, the cells were infected at a multiplicity
539 of infection (MOI) of 50:1 for *P. aeruginosa* PAO1 and PAET1 (50:1) and of 10:1 for *M. abscessus* R / S
540 and *B. thuringiensis*. Infections with each bacterium as well as coinfections combining both strains of *P.*
541 *aeruginosa* and *M. abscessus* were carried out. Three hours later, the wells were washed 3 times with
542 PBS to remove extracellular bacteria, and the plates were incubated for 24 hours. The supernatant was
543 then removed and stored at -80 °C for cytokine measurements. The effect of *P. aeruginosa*, *M. abscessus*
544 and their combination on cell viability was analyzed by Presto Blue assay (Thermo Fisher Scientific)
545 following the manufacturer's instructions, using uninfected cells as a control. Cell infections were
546 performed in triplicate in three independent experiments.
547
548 ***IL-6 and IL-8 detection by enzyme immunoassays (ELISAs) in cell supernatants***
549 IL-6 and IL-8 production was measured in cell culture supernatants using ELISA kits according to the
550 manufacturer's instructions (Becton and Dickinson, BD, San Diego, USA). Briefly, wells were coated
551 with IL-6 or IL-8 capture antibody diluted in coating buffer (0.1 M sodium carbonate, pH 9.5) overnight
552 at 4 °C. Plates were then washed and blocked with assay diluent (PBS with 10% FBS) for 1 h at room
553 temperature (RT). Plates were prepared with standards diluted in assay diluent, and samples were
554 incubated for 2 h at RT. After washing, streptavidin-horseradish peroxidase conjugate mixed with
555 biotinylated detection antibody was then added to each well for 1 h. Finally, tetramethylbenzidine (TMB)
556 substrate solution and hydrogen peroxide (BD, San Diego, USA) were added to the plates for 30 min in
557 the dark. Absorbance ($OD_{630\ nm}$) was measured in an Infinite 200 PRO microplate reader (Tecan) and
558 analyzed with Magellan software (Tecan).
559
560
561
562
563
564 **Author Contribution**
565 The manuscript was written through the contributions of all authors. Víctor Campo performed
566 the experiments. Esther Julián and Eduard Torrents directed the research, revised the
567 experimental data, and wrote the manuscript. All authors have approved the final version of the
568 manuscript.
569
570 **Acknowledgments**
571 This study was supported by grants from the Ministerio de Ciencia, Innovación y Universidades
572 and Agencia Estatal de Investigación (AEI), Spain, cofunded by Fondo Europeo de Desarrollo
573 Regional, FEDER, European Union (RTI2018-098777-B-I00, PID2021-122331OB-I00,

PID2021-125801OB-100, PDC2022-133577-I00 and PLEC2022-009356), the CERCA programme and *AGAUR-Generalitat de Catalunya* (2021SGR-0092 and 2021SGR-0145), the European Regional Development Fund (FEDER), the Catalan Cystic Fibrosis association and Obra Social "La Caixa". VC-P is a recipient of a Ph.D. contract (FI) from the Generalitat de Catalunya.

Declaration of Competing Interest

The authors declare no financial or commercial conflicts of interest.

Data Availability

The datasets used and/or analysed during the current study available from the corresponding author on reasonable request.

588 **Figure 1: Coculture of *P. aeruginosa* PAO1 and PAET1 biofilms with different bacteria. A)** Growth
589 of well-developed mature *P. aeruginosa* biofilm when different bacterial cultures (live and heat-killed) or
590 bacterial culture supernatants were added. **B)** Growth of *P. aeruginosa* in coculture biofilms. The values
591 correspond to the luciferase expression (*lux*) of the *P. aeruginosa* strains generated in each condition,
592 normalized based on the average expression reported in control wells (marked with a dashed line as 100%
593 *P. aeruginosa* growth). The effects of *M. abscessus* R and S morphotypes, *E. coli* MG1655 and *B.*
594 *thuringiensis* on both *P. aeruginosa* strains were tested as well as the supernatant (SN) and heat-killed
595 (HK) form of these bacterial cultures. Data are presented as the mean values ± SDs of at least three
596 independent experiments including six replicates in each experimental condition; significant differences
597 were determined using one-way ANOVA and Tukey's multiple comparisons tests; ****, $p < 0.0001$; ***,
598 $p < 0.001$; **, $p < 0.01$; *, $p < 0.05$. **C)** Representative confocal microscopy images of coculture biofilms
599 and pixel color quantification of the images. *P. aeruginosa* PAO1 and PAET1 biofilms were grown for 72
600 h, and *M. abscessus* R and S were inoculated for an additional 24 h. Z-stack compositions of 96 h-old *P.*
601 *aeruginosa* PAO1 and PAET1 biofilms in combination with *M. abscessus* R and S morphotypes. DAPI
602 stained all cells blue, and green fluorescent protein (GFP) of plasmid pETS218 allowed mycobacterial
603 cells to be detected in green. Scale bars correspond to 20 µm. Pixel quantifications are represented as the
604 mean values ± SDs from three representative images of each condition.

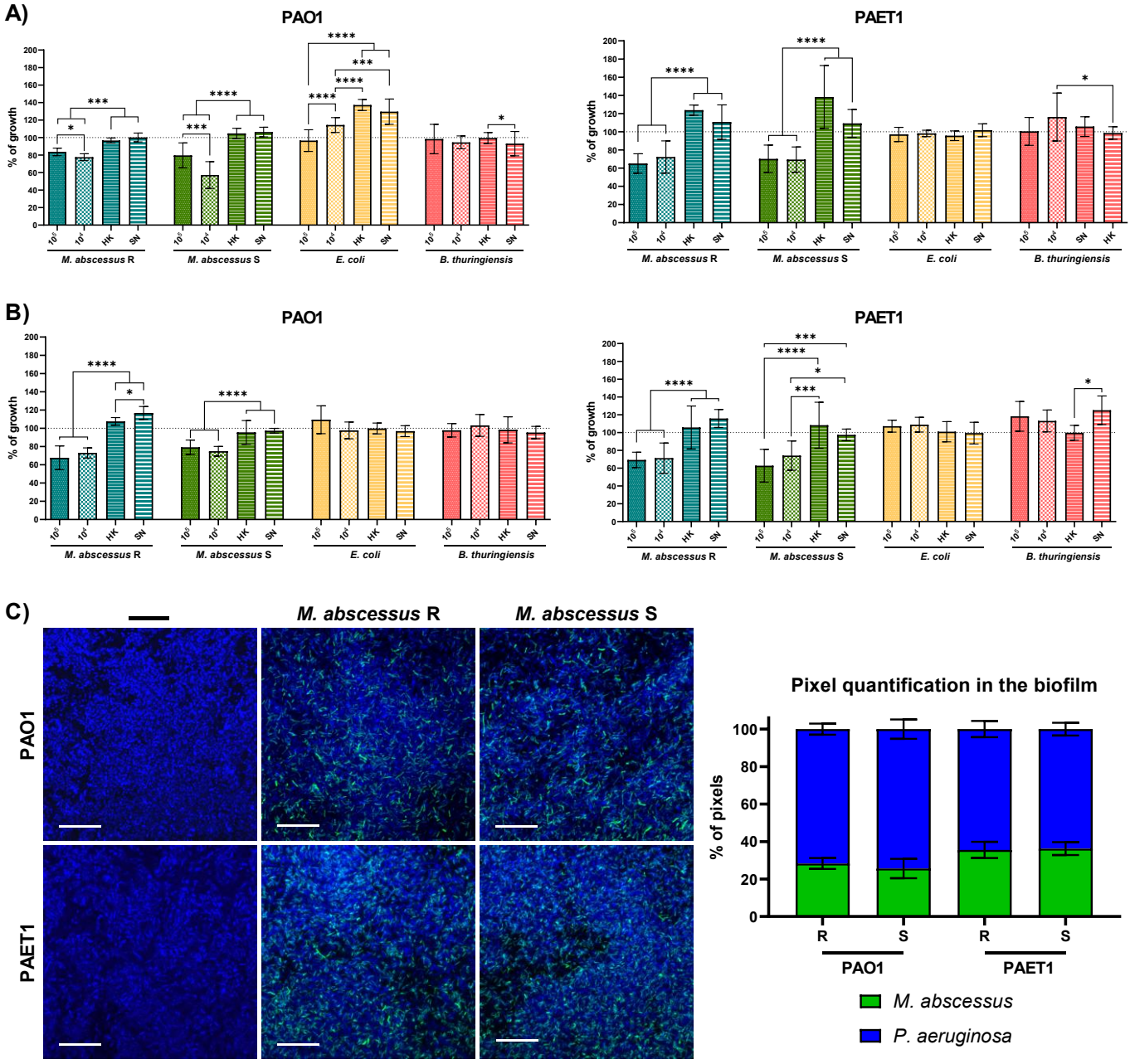
A)
PAO1
PAET1
% of growth
M. abscessus R
M. abscessus S
E. coli
B. thuringiensis
B)
C)
M. abscessus R
M. abscessus S
PAO1
PAET1
Pixel quantification in the biofilm
% of pixels
R
S
M. abscessus
P. aeruginosa

605
606
607

608 **Figure 2: Effect of the *P. aeruginosa* PAO1 and PAET1 strains on *M. abscessus* R and S biofilm**
609 **development. A)** Graph represents the inhibition of *M. abscessus* biofilms when cocultured for 72 h with
610 *P. aeruginosa* by measuring GFP expression. The control corresponds to 100% of single *M. abscessus*
611 biofilm growth by analyzing GFP expression (dotted line). Data are presented as the mean ± SD of three
612 independent experiments including six replicates in each experimental condition, and significant
613 differences were reported using the Mann–Whitney *t* test, ****, $p<0.0001$. **B)** Confocal microscopy
614 representative coculture biofilm images and pixel color quantification. Z-stack compositions of *M.*
615 *abscessus* variant 120 h biofilms in combination with *P. aeruginosa strains*. DAPI stained all cells blue,
616 and green fluorescent protein (GFP) of plasmid pETS218 allowed mycobacterial cells to be detected in
617 green. Scale bars correspond to 20 µm. Pixel quantifications are represented as the mean values ± SDs
618 from three representative images of each condition.
619

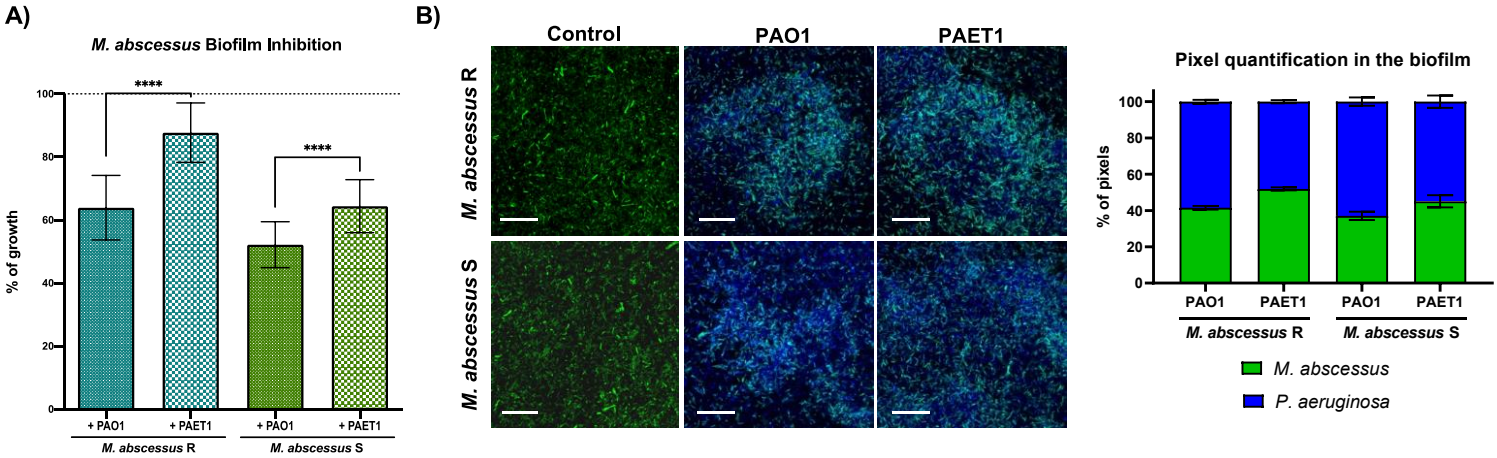

621
622

Figure 3: Bronchial epithelial cell viability and proinflammatory cytokine production after *P. aeruginosa* PAO1/PAET1, *M. abscessus* R/S and *B. thuringiensis* infections. A) Viability of CFBE41o- and 16HBE14o- cell lines after bacterial infections. Presto blue cell viability assay results in which data are expressed with respect to uninfected wells (considered as 100% cell viability). Data are represented as the mean ± SD from three independent experiments. Significance was analyzed using one-way ANOVA and Tukey's multiple comparisons test. *, $p<0.05$; **, $p<0.01$; ***, $p<0.001$; ****, $p<0.0001$. Comparison of cocultures with individual PAO1/PAET1 infections: ##, $p<0.01$; ###, $p<0.001$. **B)** Cytokine (IL-6 and IL-8) production detected in culture supernatants from bronchial epithelial cell infections. Statistical differences were determined using one-way ANOVA and Dunnett's test, which compares each column with the control. Data are represented as the mean ± SD from three independent experiments; *, $p<0.05$; **, $p<0.01$; ***, p<0.001; ****, $p<0.0001$. Comparison of results obtained in *M. abscessus* R infections and those in *M. abscessus* S infections were determined using one-way ANOVA, Tukey's multiple comparisons test; #, $p<0.05$; ##, $p<0.01$; ###, $p<0.001$; ####, $p<0.0001$.

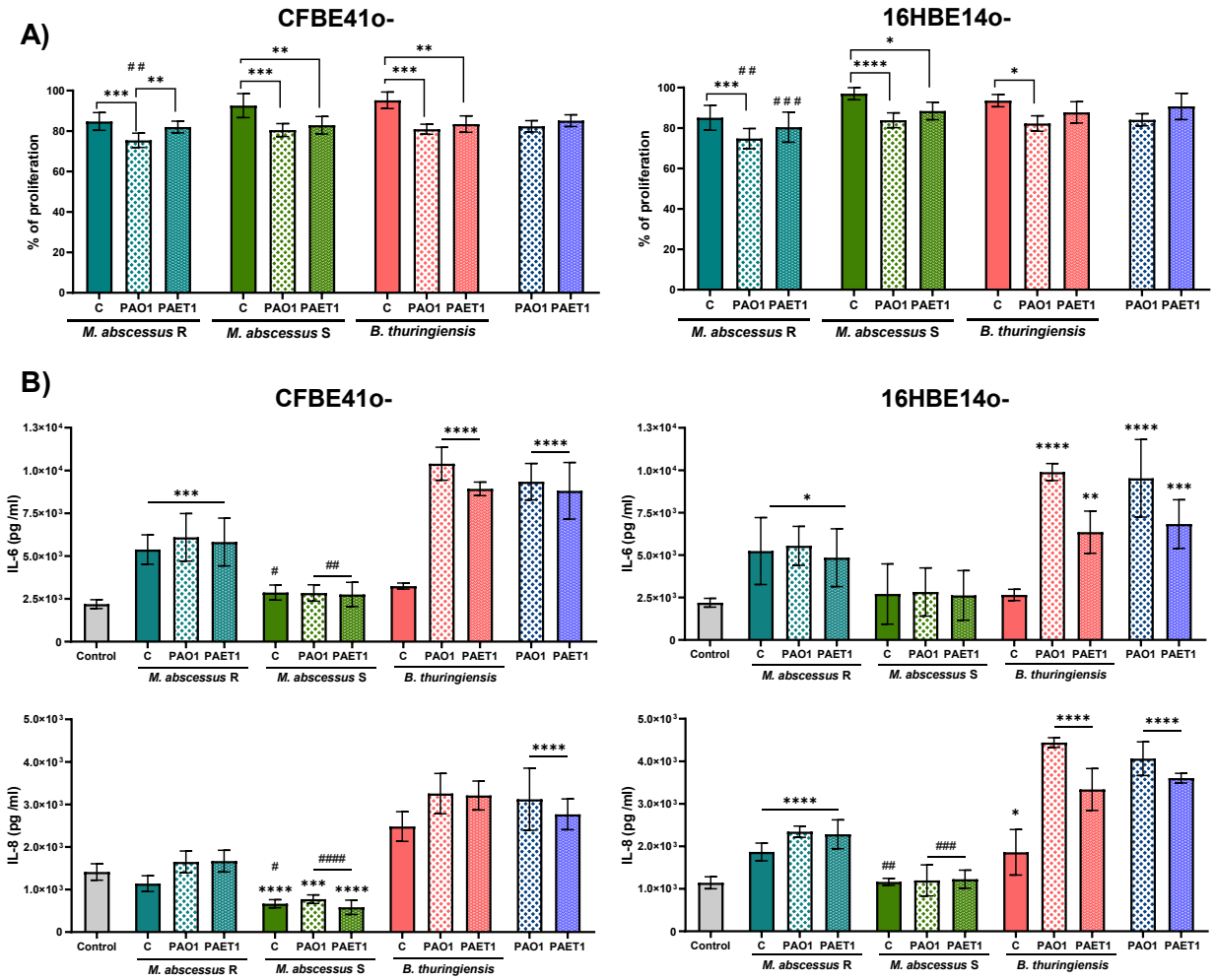

641 **Figure 4: *B. thuringiensis* and *M. abscessus* coinfecting with *P. aeruginosa* in *G. mellonella* Kaplan–**
642 **Meier survival curves**. Thirty larvae (n=30) of each condition were monitored from 12 h post-infection
643 every 2 hours to verify their survival rates when *M. abscessus* (10^4 CFU/larva) or *B. thuringiensis* (10^5
644 CFU/larva) was coinfected with *P. aeruginosa* PAO1 and PAET1 at different concentrations. Data were
645 analyzed by comparing the curves of individual *P. aeruginosa* infections with coinfection of *M. abscessus*
646 plus *P. aeruginosa* at the same concentration using the Mantel–Cox survival test; *, $p<0.05$; **, $p<0.005$.

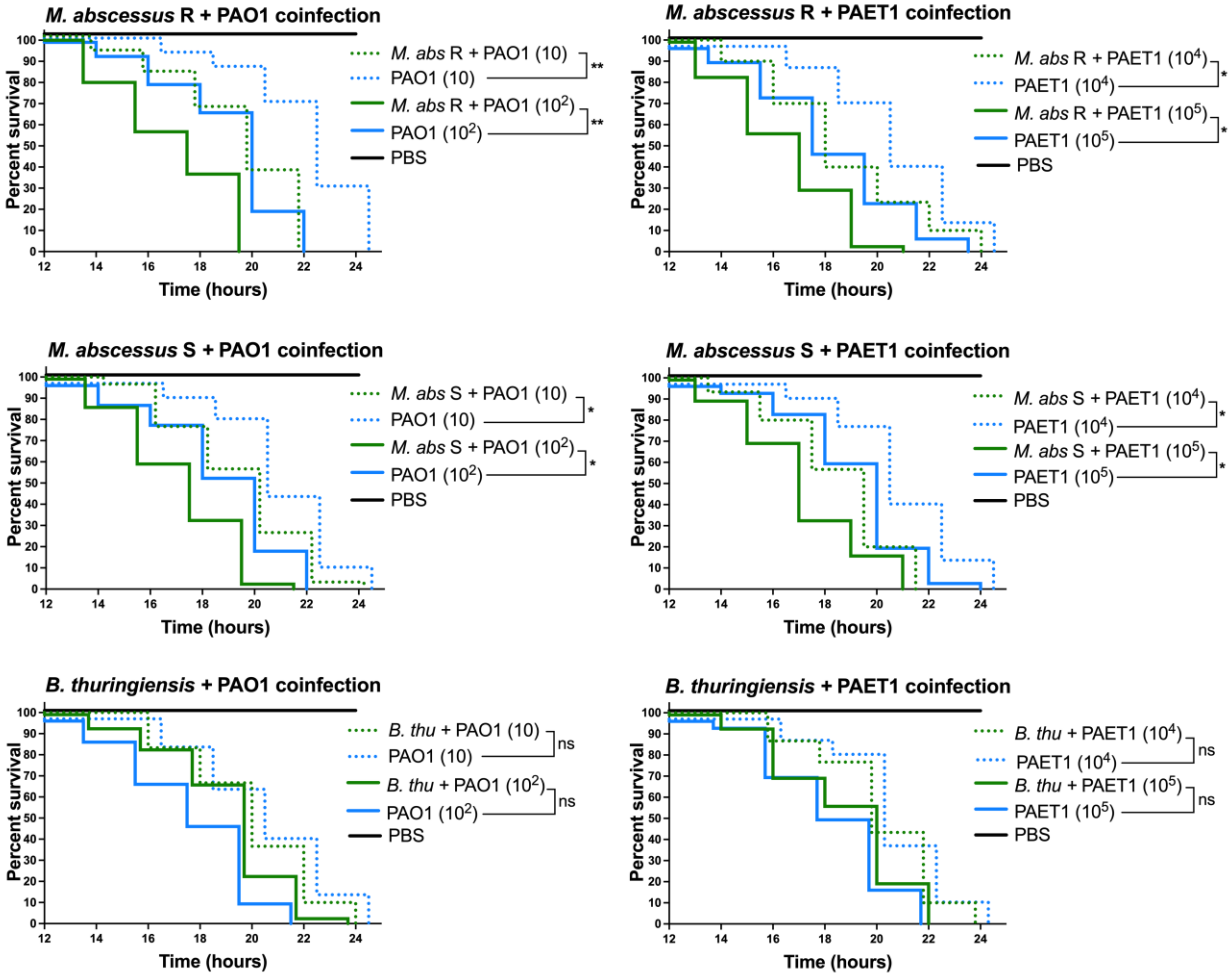

647

Figure 5: Expression of *G. mellonella* immune-relevant genes under different infection conditions. The fold changes indicate the number of times above or below the gene expression compared with the control (larvae infected with PBS) obtained by RT–PCR analysis. Data are presented as the mean ± SD of the fold changes for each condition. Significant differences were established using one-way ANOVA. *, $p<0.05$; **, $p<0.01$; **, $p<0.001$; ****, $p<0.0001$. *Apo III*: Apolipophorin III, *IMPI*: insect metalloproteinase inhibitor, *GST*: glutathione S-transferase, *NOX 4*: NADPH oxidase, *NOS*: nitric oxide synthase.

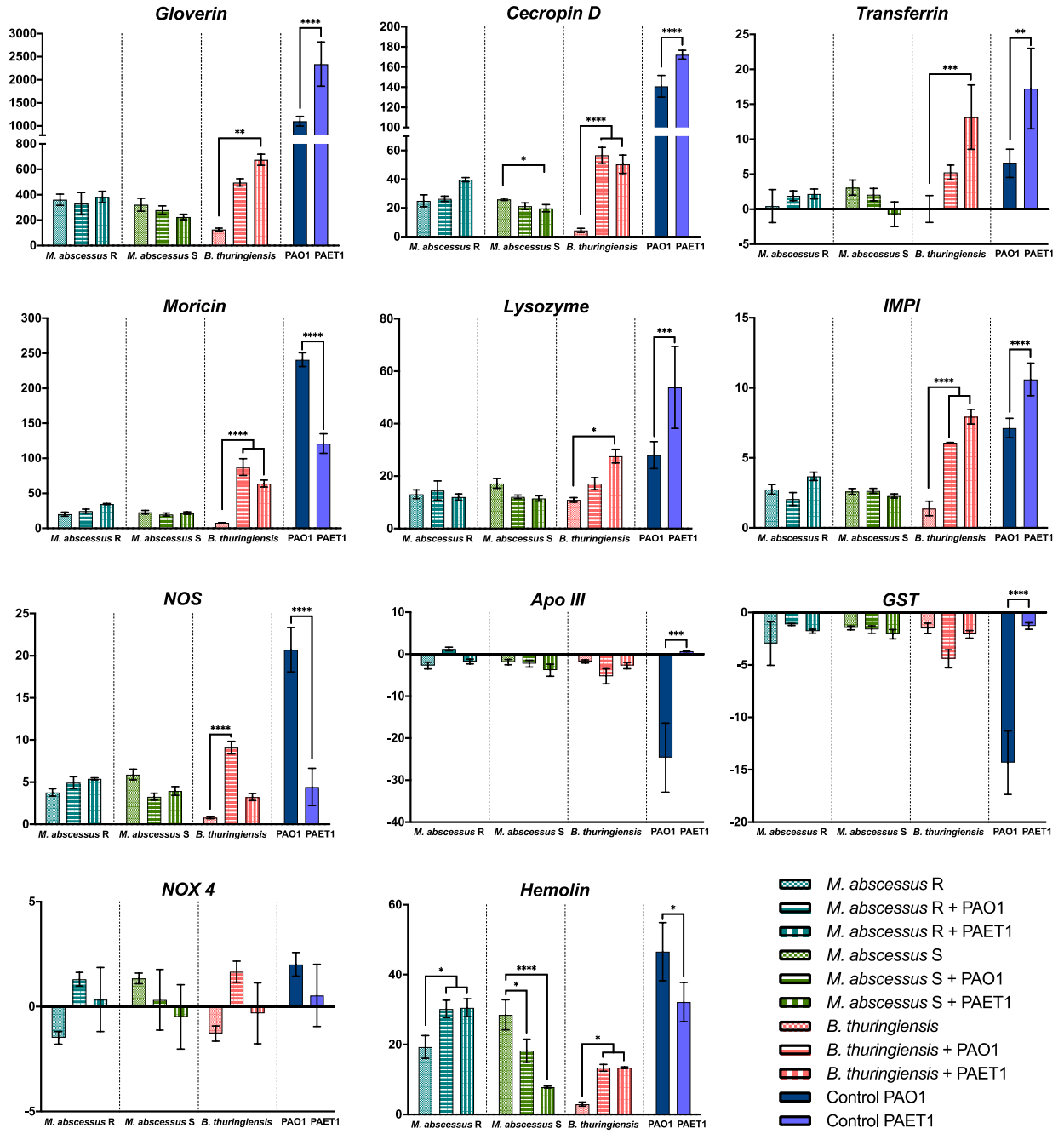

658 **References**

659 1. O'Sullivan BP, Freedman SD. 2009. Cystic fibrosis. Lancet 373:1891–1904.

660 2. Linsdell P. 2018. Cystic fibrosis transmembrane conductance regulator (CFTR): Making an ion
661 channel out of an active transporter structure. Channels (Austin) 12:284–290.

662 3. Kreda SM, Davis CW, Rose MC. 2012. CFTR, mucins, and mucus obstruction in cystic fibrosis.
663 Cold Spring Harb Perspect Med 2.

664 4. Bustamante-Marin XM, Ostrowski LE. 2017. Cilia and mucociliary clearance. Cold Spring Harb
665 Perspect Biol 9.

666 5. Coutinho H, Falcão-Silva VS, Gonçalves G. 2008. Pulmonary bacterial pathogens in cystic
667 fibrosis patients and antibiotic therapy: a tool for the health workers. Int Arch Med 1:24.

668 6. Filkins LM, O'Toole GA. 2015. Cystic fibrosis lung infections: polymicrobial, complex, and hard
669 to treat. PLoS Pathog 11:e1005258.

670 7. Jean-Pierre F, Vyas A, Hampton TH, Henson MA, O'toole GA. 2021. One versus many:
671 Polymicrobial communities and the cystic fibrosis airway. mBio 12:1–7.

672 8. Gaspar MC, Couet W, Olivier JC, Pais AACC, Sousa JJS. 2013. *Pseudomonas aeruginosa*
673 infection in cystic fibrosis lung disease and new perspectives of treatment: a review. Eur J Clin
674 Microbiol Infect Dis 32:1231–1252.

675 9. Høiby N, Ciofu O, Bjarnsholt T. 2010. *Pseudomonas aeruginosa* biofilms in cystic fibrosis. Future
676 Microbiol 5:1663–1674.

677 10. Moreau-Marquis S, Stanton BA, O'Toole GA. 2008. *Pseudomonas aeruginosa* biofilm formation
678 in the cystic fibrosis airway. Pulm Pharmacol Ther 21:595–599.

679 11. Hartl D, Gaggar A, Bruscia E, Hector A, Marcos V, Jung A, Greene C, McElvaney G, Mall M,
680 Döring G. 2012. Innate immunity in cystic fibrosis lung disease. J Cyst Fibros 11:363–382.

681 12. Martiniano SL, Nick JA, Daley CL. 2016. Nontuberculous mycobacterial infections in cystic
682 fibrosis. Clin Chest Med 37:83–96.

683 13. Abidin NZ, Gardner AI, Robinson HL, Haq IJ, Thomas MF, Brodlie M. 2021. Trends in
684 nontuberculous mycobacteria infection in children and young people with cystic fibrosis. J Cyst
685 Fibros 20:737–741.

686 14. Esther CR, Esserman DA, Gilligan P, Kerr A, Noone PG. 2010. Chronic *Mycobacterium*
687 *abscessus* infection and lung function decline in cystic fibrosis. J Cyst Fibros 9:117–123.

688 15. Brugha R, Spencer H. 2021. *Mycobacterium abscessus* in cystic fibrosis. Science 372:465–466.

689 16. Degiacomi G, Sammartino JC, Chiarelli LR, Riabova O, Makarov V, Pasca MR. 2019.
690 *Mycobacterium abscessus*, an emerging and worrisome pathogen among cystic fibrosis patients.
691 Int J Mol Sci 20.

692 17. Rodríguez-Sevilla G, Crabbé A, García-Coca M, Aguilera-Correa JJ, Esteban J, Pérez-Jorge C.
693 2019. Antimicrobial treatment provides a competitive advantage to *Mycobacterium abscessus* in a
694 dual-species biofilm with *Pseudomonas aeruginosa*. Antimicrob Agents Chemother 63.

695 18. Halloum I, Carrère-Kremer S, Blaise M, Viljoen A, Bernut A, Le Moigne V, Vilchèze C,
696 Guérardel Y, Lutfalla G, Herrmann JL, Jacobs WR, Kremer L. 2016. Deletion of a dehydratase
697 important for intracellular growth and cording renders rough *Mycobacterium abscessus* avirulent.
698 Proc Natl Acad Sci U S A 113:E4228–E4237.

699 19. Gloag ES, Wozniak DJ, Stoodley P, Hall-Stoodley L. 2021. *Mycobacterium abscessus* biofilms
700 have viscoelastic properties which may contribute to their recalcitrance in chronic pulmonary
701 infections. Sci Rep 11:5020.

20. Dokic A, Peterson E, Arrieta-Ortiz ML, Pan M, Di Maio A, Baliga N, Bhatt A. 2021. *Mycobacterium abscessus* biofilms produce an extracellular matrix and have a distinct mycolic acid profile. Cell Surf 7.

21. Gilljam M, Scherstén H, Silverborn M, Jönsson B, Ericsson Hollsing A. 2010. Lung transplantation in patients with cystic fibrosis and *Mycobacterium abscessus* infection. Journal of Cystic Fibrosis 9:272–276.

22. Thabut G, Christie JD, Mal H, Fournier M, Brugière O, Leseche G, Castier Y, Rizopoulos D. 2013. Survival benefit of lung transplant for cystic fibrosis since lung allocation score implementation. Am J Respir Crit Care Med 187:1335–1340.

23. Maurice NM, Bedi B, Sadikot RT. 2018. *Pseudomonas aeruginosa* biofilms: host response and clinical implications in lung infections. Am J Respir Cell Mol Biol 58:428–439.

24. Esteban J, García-Coca M. 2018. Mycobacterium Biofilms. Front Microbiol 8.

25. Shokri D, Khorasgani MR, Mohkam M, Fatemi SM, Ghasemi Y, Taheri-Kafrani A. 2018. The inhibition effect of *Lactobacilli* against growth and biofilm formation of *Pseudomonas aeruginosa*. Probiotics Antimicrob Proteins 10:34–42.

26. Reece E, Doyle S, Greally P, Renwick J, McClean S. 2018. *Aspergillus fumigatus* inhibits *Pseudomonas aeruginosa* in co-culture: implications of a mutually antagonistic relationship on virulence and inflammation in the CF airway. Front Microbiol 9.

27. Birmes FS, Wolf T, Kohl TA, Rüger K, Bange F, Kalinowski J, Fetzner S. 2017. *Mycobacterium abscessus subsp. abscessus* is capable of degrading *Pseudomonas aeruginosa* quinolone signals. Front Microbiol 8.

28. Cortes MAM, Nessar R, Singh AK. 2010. Laboratory maintenance of *Mycobacterium abscessus*. Curr Protoc Microbiol Chapter 10.

29. LaBauve AE, Wargo MJ. 2012. Growth and laboratory maintenance of *Pseudomonas aeruginosa*. Curr Protoc Microbiol Chapter 6.

30. Rodríguez-Sevilla G, García-Coca M, Romera-García D, Aguilera-Correa JJ, Mahíllo-Fernández I, Esteban J, Pérez-Jorge C. 2018. Non-Tuberculous Mycobacteria multispecies biofilms in cystic fibrosis: development of an in vitro *Mycobacterium abscessus* and *Pseudomonas aeruginosa* dual species biofilm model. Int J Med Microbiol 308:413–423.

31. Idosa AW, Wozniak DJ, Hall-Stoodley L. 2022. Surface dependent inhibition of *Mycobacterium abscessus* by diverse *Pseudomonas aeruginosa* strains. Microbiol Spectr 10.

32. Clary G, Sasindran SJ, Nesbitt N, Mason L, Cole S, Azad A, McCoy K, Schlesinger LS, Hall-Stoodley L. 2018. *Mycobacterium abscessus* smooth and rough morphotypes form antimicrobial-tolerant biofilm phenotypes but are killed by acetic acid. Antimicrob Agents Chemother 62.

33. Bernut A, Herrmann JL, Kissa K, Dubremetz JF, Gaillard JL, Lutfalla G, Kremer L. 2014. *Mycobacterium abscessus* cording prevents phagocytosis and promotes abscess formation. Proc Natl Acad Sci U S A 111.

34. De Groote MA, Huitt G. 2006. Infections due to rapidly growing mycobacteria. Clin Infect Dis 42:1756–1763.

35. Del Mar Cendra M, Torrents E. 2020. Differential adaptability between reference strains and clinical isolates of *Pseudomonas aeruginosa* into the lung epithelium intracellular lifestyle. Virulence 11:862–876.

36. Hsieh MH, Lin CY, Wang CY, Fang YF, Lo YL, Lin SM, Lin HC. 2018. Impact of concomitant nontuberculous mycobacteria and *Pseudomonas aeruginosa* isolates in non-cystic fibrosis bronchiectasis. Infect Drug Resist 11:1137–1143.

37. Brennan MJ. 2017. Biofilms and *Mycobacterium tuberculosis*. Infect Immun 85.

748 38. Courtney JM, Ennis M, Elborn JS. 2004. Cytokines and inflammatory mediators in cystic fibrosis.
749 J Cyst Fibros 3:223–231.

750 39. Roesch EA, Nichols DP, Chmiel JF. 2018. Inflammation in cystic fibrosis: An update. Pediatr
751 Pulmonol 53:S30–S50.

752 40. Kube D, Sontich U, Fletcher D, Davis PB. 2001. Proinflammatory cytokine responses to *P.*
753 *aeruginosa* infection in human airway epithelial cell lines. Am J Physiol Lung Cell Mol Physiol
754 280.

755 41. Gangell C, Gard S, Douglas T, Park J, De Klerk N, Keil T, Brennan S, Ranganathan S, Robins-
756 Browne R, Sly PD. 2011. Inflammatory responses to individual microorganisms in the lungs of
757 children with cystic fibrosis. Clin Infect Dis 53:425–432.

758 42. Heijerman H. 2005. Infection and inflammation in cystic fibrosis: a short review. J Cyst Fibros 4
759 Suppl 2:3–5.

760 43. Bertelsen A, Elborn JS, Schock BC. 2021. Microbial interaction: *Prevotella spp.* reduce *P.*
761 *aeruginosa* induced inflammation in cystic fibrosis bronchial epithelial cells. J Cyst Fibros
762 20:682–691.

763 44. Le Moigne V, Roux AL, Jobart-Malfait A, Blanc L, Chaoui K, Burlet-Schiltz O, Gaillard JL,
764 Canaan S, Nigou J, Herrmann JL. 2020. A TLR2-Activating fraction from *Mycobacterium*
765 *abscessus* rough variant demonstrates vaccine and diagnostic potential. Front Cell Infect Microbiol
766 10.

767 45. Kempaiah P, Davidson LB, Perkins DJ, Byrd TF. 2013. Cystic fibrosis CFBE41o- cells contain
768 TLR1 SNP I602S and fail to respond to *Mycobacterium abscessus*. J Cyst Fibros 12:773.

769 46. Davidson LB, Nessar R, Kempaiah P, Perkins DJ, Byrd TF. 2011. *Mycobacterium abscessus*
770 Glycopeptidolipid prevents respiratory epithelial TLR2 signaling as measured by HβD2 gene
771 expression and IL-8 release. PLoS One 6:29148.

772 47. van Heeckeren AM, Sutton MT, Fletcher DR, Hodges CA, Caplan AI, Bonfield TL. 2021.
773 Enhancing cystic fibrosis immune regulation. Front Pharmacol 12.

774 48. Jander G, Rahme LG, Ausubel FM. 2000. Positive correlation between virulence of *Pseudomonas*
775 *aeruginosa* mutants in mice and insects. J Bacteriol 182:3843–3845.

776 49. Ramarao N, Nielsen-Leroux C, Lereclus D. 2012. The insect *Galleria mellonella* as a powerful
777 infection model to investigate bacterial pathogenesis. J Vis Exp https://doi.org/10.3791/4392.

778 50. Harrison EM, Carter MEK, Luck S, Ou HY, He X, Deng Z, O'Callaghan C, Kadioglu A,
779 Rajakumar K. 2010. Pathogenicity islands PAPI-1 and PAPI-2 contribute individually and
780 synergistically to the virulence of *Pseudomonas aeruginosa* strain PA14. Infect Immun 78:1437–
781 1446.

782 51. Meir M, Grosfeld T, Barkan D. 2018. Establishment and validation of *Galleria mellonella* as a
783 novel model organism to study *Mycobacterium abscessus* infection, pathogenesis, and treatment.
784 Antimicrob Agents Chemother 62.

785 52. Li Y, Spiropoulos J, Cooley W, Khara JS, Gladstone CA, Asai M, Bossé JT, Robertson BD,
786 Newton SM, Langford PR. 2018. *Galleria mellonella* - a novel infection model for the
787 *Mycobacterium tuberculosis* complex. Virulence 9:1126–1137.

788 53. Andrejko M, Mak P, Siemińska-Kuczer A, Iwański B, Wojda I, Suder P, Kuleta P, Regucka K,
789 Cytryńska M. 2021. A comparison of the production of antimicrobial peptides and proteins by
790 *Galleria mellonella* larvae in response to infection with two *Pseudomonas aeruginosa* strains
791 differing in the profile of secreted proteases. J Insect Physiol 131.

792 54. Xu XX, Zhong X, Yi HY, Yu XQ. 2012. *Manduca sexta* gloverin binds microbial components and
793 is active against Bacteria and Fungi. Dev Comp Immunol 38:275.

794 55. Yi HY, Chowdhury M, Huang YD, Yu XQ. 2014. Insect antimicrobial peptides and their
795 applications. Appl Microbiol Biotechnol 98:5807–5822.

796 56. Moore AJ, Beazley WD, Bibby MC, Devine DA. 1996. Antimicrobial activity of cecropins. J
797 Antimicrob Chemother 37:1077–1089.

798 57. Hara S, Yamakawa M. 1995. Moricin, a novel type of antibacterial peptide isolated from the
799 silkworm, *Bombyx moriv*. J Biol Chem 270:29923–29927.

800 58. Vertyporokh L, Wojda I. 2017. Expression of the insect metalloproteinase inhibitor IMPI in the fat
801 body of *Galleria mellonella* exposed to infection with *Beauveria bassiana*. Acta Biochim Pol
802 64:273–278.

803 59. Wojda I. 2017. Immunity of the greater wax moth *Galleria mellonella*. Insect Sci 24:342–357.

804 60. Galdino ACM, Branquinha MH, Santos ALS, Viganor L. 2017. *Pseudomonas aeruginosa* and its
805 arsenal of proteases: Weapons to battle the host. Pathophysiological Aspects of Proteases 381–
806 397.

807 61. Clermont A, Wedde M, Seitz V, Podsiadlowski L, Lenze D, Hummel M, Vilcinskas A. 2004.
808 Cloning and expression of an inhibitor of microbial metalloproteinases from insects contributing
809 to innate immunity. Biochemical Journal 382:315.

810 62. Fallon JP, Troy N, Kavanagh K. 2011. Pre-exposure of *Galleria mellonella* larvae to different
811 doses of *Aspergillus fumigatus* conidia causes differential activation of cellular and humoral
812 immune responses. Virulence 2:413–421.

813 63. Catalão MJ, Pimentel M. 2018. Mycobacteriophage lysis enzymes: targeting the mycobacterial
814 cell envelope. Viruses 10.

815 64. Rao XJ, Ling E, Yu XQ. 2010. The role of lysozyme in the prophenoloxidase activation system of
816 *Manduca sexta*: an in vitro approach. Dev Comp Immunol 34:264–271.

817 65. Iatsenko I, Marra A, Boquete JP, Peña J, Lemaitre B. 2020. Iron sequestration by transferrin 1
818 mediates nutritional immunity in *Drosophila melanogaster*. Proc Natl Acad Sci U S A 117:7317–
819 7325.

820 66. Minandri F, Imperi F, Frangipani E, Bonchi C, Visaggio D, Facchini M, Pasquali P, Bragonzi A,
821 Visca P. 2016. Role of iron uptake systems in *Pseudomonas aeruginosa* virulence and airway
822 infection. Infect Immun 84:2324–2335.

823 67. Sadekuzzaman M, Stanley D, Kim Y. 2018. Nitric oxide mediates insect cellular immunity via
824 phospholipase A2 activation. J Innate Immun 10:70–81.

825 68. Hillyer JF, Estévez-Lao TY. 2010. Nitric oxide is an essential component of the hemocyte-
826 mediated mosquito immune response against bacteria. Dev Comp Immunol 34:141–149.

827 69. Vogel H, Altincicek B, Glöckner G, Vilcinskas A. 2011. A comprehensive transcriptome and
828 immune-gene repertoire of the lepidopteran model host *Galleria mellonella*. BMC Genomics
829 12:1–19.

830 70. Lu A, Zhang Q, Zhang J, Yang B, Wu K, Xie W, Luan YX, Ling E. 2014. Insect
831 prophenoloxidase: the view beyond immunity. Front Physiol 5.

832 71. Zakarian RJ, Dunphy GB, Albert PJ, Rau ME. 2002. Apolipophorin-III affects the activity of the
833 haemocytes of *Galleria mellonella* larvae. J Insect Physiol 48:715–723.

834 72. Andrejko M, Mizerska-Dudka M, Jakubowicz T. 2008. Changes in *Galleria mellonella*
835 apolipophorin III level during *Pseudomonas aeruginosa* infection. J Invertebr Pathol 97:14–19.

836 73. Andrejko M, Cytryńska M, Jakubowicz T. 2005. Apolipophorin III is a substrate for protease IV
837 from *Pseudomonas aeruginosa*. FEMS Microbiol Lett 243:331–337.

838 74. Bergin D, Reeves EP, Renwick J, Wientjes FB, Kavanagh K. 2005. Superoxide production in
839 *Galleria mellonella* hemocytes: identification of proteins homologous to the NADPH oxidase
840 complex of human neutrophils. Infect Immun 73:4161–4170.

841 75. Admella J, Torrents E. 2023. Investigating bacterial infections in *Galleria mellonella* larvae:
842 Insights into pathogen dissemination and behavior. J Invertebr Pathol 200.

843 76. Malhotra S, Hayes D, Wozniak DJ. 2019. Cystic fibrosis and *Pseudomonas aeruginosa*: the host-
844 microbe interface. Clin Microbiol Rev 32.

845 77. Dinwiddie R. 2005. Anti-inflammatory therapy in cystic fibrosis. J Cyst Fibros 4 Suppl 2:45–48.

846 78. Caverly LJ, Caceres SM, Fratelli C, Happoldt C, Kidwell KM, Malcolm KC, Nick JA, Nichols
847 DP. 2015. *Mycobacterium abscessus* morphotype comparison in a murine model. PLoS One 10.

848 79. Crespo A, Gavaldà J, Julián E, Torrents E. 2017. A single point mutation in class III
849 ribonucleotide reductase promoter renders *Pseudomonas aeruginosa* PAO1 inefficient for
850 anaerobic growth and infection. Sci Rep 7.

851 80. Moya-Andérico L, Admella J, Fernandes R, Torrents E. 2020. Monitoring gene expression during
852 a *Galleria mellonella* bacterial infection. Microorganisms 8:1–14.

853 81. Brambilla C, Llorens-Fons M, Julián E, Noguera-Ortega E, Tomàs-Martínez C, Pérez-Trujillo M,
854 Byrd TF, Alcaide F, Luquin M. 2016. Mycobacteria clumping increase their capacity to damage
855 macrophages. Front Microbiol 7:1562.

856 82. Campo-Pérez V, Cendra M del M, Julián E, Torrents E. 2021. Easily applicable modifications to
857 electroporation conditions improve the transformation efficiency rates for rough morphotypes of
858 fast-growing mycobacteria. N Biotechnol 63:10–18.

859 83. Falcon I. 1982. Molecular cloning: A laboratory manual third edition. Molecular Cloning: A
860 Laboratory Manual Third Edition.

861 84. Perrone F, De Siena B, Muscariello L, Kendall SL, Waddell SJ, Sacco M. 2017. A novel TetR-like
862 transcriptional regulator is induced in acid-nitrosative stress and controls expression of an efflux
863 pump in Mycobacteria. Front Microbiol 8.

864 85. Campo-Pérez V, Alcàcer-Almansa J, Julián E, Torrents E. 2023. A high-throughput microtiter
865 plate screening assay to quantify and differentiate species in dual-species biofilms.
866 Microorganisms 2023, Vol 11, Page 2244 11:2244.

867